zian,

$$d^2\sigma/d\Omega d\omega \propto |F|^2 \mathrm{Im}(\omega - \langle \omega_s + \omega_{NP} + \omega_D \rangle - i\Gamma)^{-1}, \quad (4)$$

where $\Gamma = \tau_p[\langle(\omega_{NP}+\omega_D)^2\rangle - \langle \omega_{NP}+\omega_D\rangle^2]$. Note that the resonance is at the average spin excitation energy and the linewidth is directly proportional to τ_p.

With the inclusion of orbital collisions in the line-shape theory there is qualitative agreement between theory and experiment for the linewidth as a function of magnetic field, the general features of the line shapes, and the relative peak positions in the two geometries. Further extensions of both the theoretical and the experimental results are necessary before a quantitative comparison of theory and experiment for the details of the line shape can be carried out. Resonance-enhancement effects[5] which make the spin-flip matrix element F dependent on k_z should be included. Improvement in the resolution is also necessary, particularly in the $\vec{q}\cdot\vec{H}=0$ geometry. Only qualitative observations of the effects of varying temperature and electron concentration have been made and are reported elsewhere.[5] A microscopic theoretical treatment of the line shape is clearly desirable. Some work on this problem is presently being carried out.[12,13]

We wish to acknowledge helpful discussions with A. Mooradian, A. L. McWhorter, R. W. Davies, Y. C. Auyang, and P. A. Wolff, and the expert technical assistance of D. J. Wells.

†Work sponsored by the U. S. Department of the Air Force.

[1]C. K. N. Patel and E. D. Shaw, Phys. Rev. 24, 451 (1970); C. K. N. Patel, Appl. Phys. Lett. 19, 400 (1971).

[2]A. Mooradian, S. R. J. Brueck, and F. A. Blum, Appl. Phys. Lett. 17, 481 (1970); S. R. J. Brueck and A. Mooradian, *ibid.* 18, 229 (1971).

[3]R. L. Allwood, S. D. Devine, R. G. Mellish, S. D. Smith, and R. A. Wood, J. Phys. C: Proc. Phys. Soc., London 3, L186 (1970); R. G. Mellish, R. B. Dennis, and R. L. Allwood, Opt. Commun. 4, 249 (1971).

[4]R. B. Aggarwal, B. Lax, C. E. Chase, C. R. Pidgeon, D. Limbert, and F. Brown, Appl. Phys. Lett. 18, 383 (1971).

[5]S. R. J. Brueck and A. Mooradian, Phys. Rev. Lett. 28, 161 (1972); S. R. J. Brueck, Ph. D. thesis, Massachusetts Institute of Technology, 1971 (unpublished).

[6]R. W. Davies and F. A. Blum, Phys. Rev. B 3, 3321 (1971).

[7]F. A. Blum, Phys. Rev. B 1, 1125 (1970).

[8]For simplicity, only the leading terms of each contribution to ω_{NP} and ω_D will be noted in the test. In performing the comparison between theory and experiment it is important to use more accurate expressions for the energy differences correct to second order in the small quantities $\hbar^2 k_z^2/m_c E_g$ and $\hbar^2 s/m_c E_g$ where $s = eH/\hbar c$ (cf. Ref. 5).

[9]The measured dc Hall mobility in the material used in these experiments is $\mu \approx 1.3\times10^5$ cm^2/V sec which gives a collision time of 10^{-12} sec.

[10]R. A. Isaacson, Phys. Rev. 169, 312 (1968); E. M. Gershenzon, N. M. Perin, and M. S. Fogel'son, Fiz. Tverd. Tela 10, 2880 (1968) [Sov. Phys. Solid State 10, 2278 (1969)].

[11]See, for example, C. P. Slichter, *Principles of Magnetic Resonance* (Harper and Row, New York, 1964), Chap. 5.

[12]Y. C. Auyang and P. A. Wolff, private communication; Y. C. Auyang, Ph. D. thesis, Massachusetts Institute of Technology, 1971 (unpublished).

[13]R. W. Davies, private communication.

Observation of Second Sound in Bismuth

V. Narayanamurti and R. C. Dynes
Bell Laboratories, Murray Hill, New Jersey 07974
(Received 10 April 1972)

We have observed the transition from ballistic to second sound to diffusive propagation of heat (phonon) pulses in the semimetal bismuth in the temperature range of 1.2 to 4.0 K. The saturated second-sound velocity is found to be independent of orientation and has a a value of $(0.78\pm0.05)\times10^5$ cm/sec ($\frac{1}{3}\sqrt{3}$ times the Debye velocity). The inverse of the normal process phonon lifetime has a value $\tau_N^{-1} = 4.49\times10^4 T^4$ sec^{-1}. Scattering due to the hole-phonon interaction is observed for ballistic L modes propagating along the C_3 axis.

In a pure dielectric solid, depending upon the temperature, heat can propagate without interaction (ballistic phonons), as a true temperature wave (collective second sound), or by diffusion. In this paper we report our observation of the transition from ballistic to second sound to diffusive heat propagating in bismuth and show that the saturated second-sound velocity (at ~3.5 K) is the same for all three orthogonal axes. The results indicate that the collective second-sound mode is probably a true thermodynamic average of all the different modes of the multiple polariza-

tion system. In addition, we measure the orientation dependence of the intensities of the ballistic pulses (at ~1.3 K), and present evidence for hole-phonon scattering for L modes propagating along the threefold axis.

Because of its unique properties as a semimetal with a relatively low Debye temperature Θ, the electrical and vibrational properties of bismuth have been extensively studied in the past. Because of the relatively low carrier concentration ($n_e \approx n_h \approx 3\times10^{17}/\mathrm{cm}^3$), the dominant mechanism for thermal conduction at low temperature is via the phonons.[1] The isotopic purity and high degree of chemical and physical perfection of single-crystal bismuth make it a prime candidate for the observation of second sound in a material other than a dielectric solid.[2] This fact has been reiterated most recently in the low-temperature thermal-conductivity measurements of Kopylov and Mezhov-Deglin.[3] The conditions for second-sound propagation and observation have been well documented theoretically,[4] but experimentally the only solids to display this mode of heat propagation to date are helium[5] and sodium fluoride.[6] In He this experiment has not been attempted at temperatures low enough to see complete ballistic flow,[7] while in NaF the saturation of the velocity in the second-sound regime has not been observed because of the onset of resistive (probably intrinsic) scattering processes. In addition, the orientation dependence has not been studied in either of these materials. Bismuth is a very anisotropic solid elastically. The prospect of observing second sound directly and probing its evolution from the different ballistic modes as a function of orientation in a highly anisotropic medium, and the possibility of observing aspects of the electron (hole) -phonon interaction motivated our heat-pulse work in Bi.

The Bi crystals studied were zone refined and displayed electrical resistance ratios $R(300\ \mathrm{K})/R(4.2\ \mathrm{K})$ from 100 to 400. The crystals were acid-string saw cut to avoid strain, and the surfaces were polished very gently using an electromechanical etch. Insulating films of Ge and/or SiO were evaporated onto opposite surfaces. A Constantan heater (~1000 Å thick) was deposited on one end and a superconducting Pb bolometer (~1000 Å) on the opposite face. A magnetic field of up to 1 kG was used to bias the bolometer. Great care was taken to cool the sample slowly (from 300 to 77 K over 8 h) and the sample was hung from only one point to avoid strain. The submicrosecond heat pulses were generated and detected using standard techniques.[8]

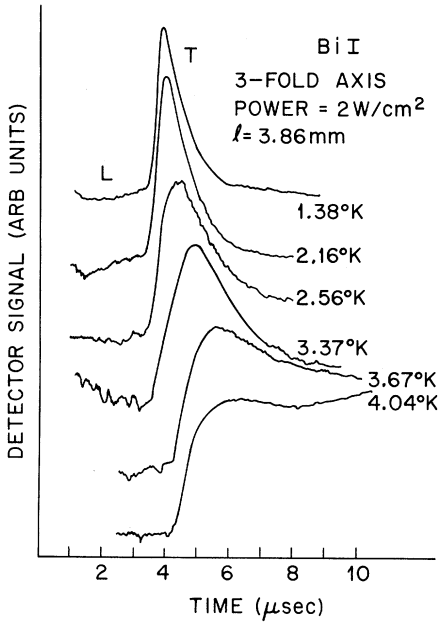

FIG. 1. Heat pulses in Bi along the C_3 axis.

Figure 1 shows the temperature dependence of heat-pulse propagation along the C_3 axis over a distance of 3.86 mm. The input pulse powers, for the data reported here, were small, and the temperature rise above ambient at the heater was typically less than 0.1 K.

At 1.38 K the arrival of a pulse corresponding to ballistic propagation of a transverse phonon group in this direction is clearly observed and is labeled T. The velocity of this degenerate T mode is in good agreement with ultrasonic measurements[9] and confirms that we are, in fact, seeing ballistic transverse-phonon propagation. At earlier times where one would expect the arrival of the longitudinal mode (L), careful study of the data suggests that there is the slight hint of a pulse, but it is more diffusive than ballistic in nature, i.e., the signal rises at the expected ballistic arrival time but keeps increasing rather than reflecting the pulse shape. This lack of L mode (in a direction where we expect strong L-mode focusing) is due, we believe, to hole-phonon scattering. We will return to this point shortly.

As the temperature was raised to 3.5 K, a broadening of the pulse was observed and a delayed arrival of the peak position resulted (Fig. 1). Above this temperature the result of resistive processes became apparent as the pulse lost its form and the peak was further retarded in time. This higher-temperature dependence of

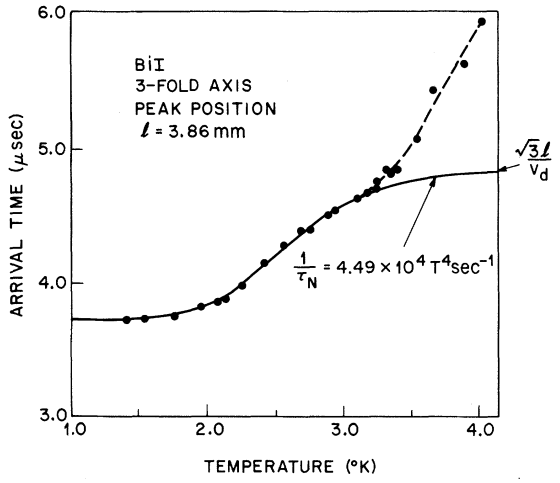

FIG. 2. Arrival time of the peak position as a function of temperature from the data of Fig. 1. Solid line, calculated from the dispersion relation for second sound (see text).

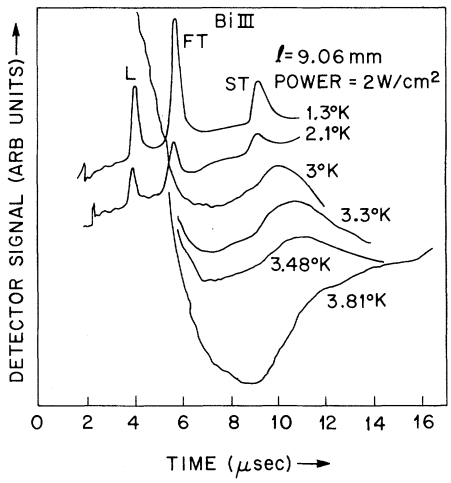

FIG. 3. Heat pulses in Bi along the twofold axis.

the heat pulse was consistent with the thermal-conductivity data[3] which exhibited dominant umklapp scattering above 3.5 K.

It is the time retardation and broadening of the pulse below 3.5 K with maintainance of true pulselike behavior that we associate with the onset of second-sound propagation. In Fig. 2 the arrival time of the *peak* of the pulse is plotted as a function of ambient temperature. It is seen that the arrival time begins to saturate at about 3 K. Assuming a plane-wave solution for temperature propagation in the second-sound regime ($T = T_0 e^{i(kx-\omega t)}$) and defining a "second viscosity" in analogy with hydrodynamics, the heat-flow equation can be solved and the dispersion relation for the resulting temperature wave is[4,6]

$$k^2 C_2^2 = \omega^2 + \frac{i\omega}{\tau_R} - \frac{i\omega k^2 \tau (C_1^2 - C_2^2)}{1 - i\omega\tau}, \qquad (1)$$

with $\tau^{-1} = \tau_R^{-1} + \tau_N^{-1}$ and where C_2 is the second-sound velocity, C_1 is the ballistic phonon velocity (assuming single-mode propagation), τ_R is the resistive scattering time, and τ_N the normal-process scattering time. The real and imaginary parts of k determine the phase velocity and the attenuation of the wave, respectively. From this equation it is clear that the conditions for observations of unattenuated second sound are $C_1\tau_N \ll l$ and $C_1\tau_R \gg l$, where l is the propagation length.

Employing this dispersion relation and for simplicity assuming in the region 1.5–3.3 K that $\tau_R = \infty$, the experimental value for τ_N has been calculated from the velocity profile of Fig. 2. The saturated second-sound velocity C_2 was found to be $v_d/\sqrt{3} = 0.78 \times 10^5$ cm/sec where v_d is calculated from the 0 K value[10] of Θ (120 K). A best fit to the velocity-profile data (solid line of Fig. 2) was obtained using (1) and with $\tau_N^{-1} = 4.49 \times 10^4 T^{4\pm0.3}$. It should be emphasized that this value of τ_N is strictly valid for the T modes in the C_3 direction, although the T^4 dependence is believed to hold for all modes. The estimate of τ_N from thermal-conductivity data[11] indicates a similar temperature dependence but an average numerical value some 7 times smaller than our heat-pulse analysis for the T modes. The temperature dependence observed by us is close to that found by Rogers[6] for NaF, but is faster than the T^{-3} dependence for τ_N found by Ackerman and Guyer[4] for solid He^4. Theoretically, Herring[12] has predicted an ωT^4 dependence for τ_N^{-1} for subthermal phonons. Measurements of the explicit ω dependence are planned.

The results for propagation in the twofold axis over a distance of $l = 9.06$ mm are shown in Fig. 3. Unlike the C_3-axis results, at the lowest temperatures we observed the ballistic propagation of all three modes. Note the large velocity difference between the two transverse modes. As the temperature was raised, *all three* ballistic modes decreased rapidly in intensity as a result of phonon decay by N processes. By 3 K most of this intensity was transformed into a new peak, the second-sound mode, propagating at a velocity slightly slower than ST. This observation indicated that the second-sound pulse consisted of a true thermodynamic mixture of all the modes of the system. This was further borne out by the

fact that the saturated second-sound velocity (at ~3.4 K) was again found, within experimental error, to be equal to $C_2 = v_d/\sqrt{3} = 0.78\times10^5$ cm/sec. At high temperatures, (>3.5 K), the diffusion pulse, as in the C_3 axis, began to dominate the data.

The results in the bisectrix direction, although different in detail, displayed qualitatively similar behavior to that in Fig. 3 with all three modes again decaying into a second-sound mode in the vicinity of 3 K with the same velocity as above. The orientation dependence reported here has been seen both in the same sample and in three different samples. In addition, in all directions we observed the pulses on a long background tail as is evident in Fig. 3. This we ascribe to electronic effects associated with measurements on metallic crystals, but the details are not presently understood.

The question arises as to why the L mode is absent in the C_3-axis results. We believe this is because of hole-phonon interactions. It has been shown that the frequency spectrum of phonons emitted from a heater is blackbody in nature[13] and can be simply described in terms of a characteristic heater temperature T_h. For a heat pulse of 2 K, the average L-phonon wave vector q is 4.5×10^6 cm^{-1}. The caliper dimensions of the hole surface[14] (assuming it to be an ellipsoid) are given as $2k_1 = 2k_2 = 2.74\times10^6$ cm^{-1}, while $2k_3 = 9.4\times10^6$ cm^{-1}. Hence, for phonons propagating in the C_3 axis, scattering is possible, while orthogonal to this direction, conservation of momentum disallows the process. In addition, we know that the L-phonon mean free path λ_L is given approximately by[15]

$$1/\lambda_L = (m^*)^2 E_u^2 \nu/\zeta c_L^2 \hbar^3, \qquad (2)$$

where ζ is the mass density, m^* is the effective mass of the scattered holes, ν is the phonon frequency, and E_u is the deformation potential. For values of $m^* = 0.2m_e$ and $E_u = 6.5$ eV this gives a λ_L in the C_3 axis of the order of 0.01 mm, not inconsistent with our results.

In the bisectrix direction we expect electron–L-phonon scattering. The electron surface is an ellipsoid tilted 6° 20′ from this direction. Using an appropriate effective mass ($\sim 0.01 m_e$) for phonon scattering by a 2-K heat pulse, one obtains an L-phonon mean free path ~4mm, and not inconsistent with our data. Because of the shapes of the electron and hole surfaces, L-phonon scattering in other directions is expected to be very weak. Of course, since the phase space for umklapp scattering is so small, we do not expect to see T-phonon scattering in any direction. Because of the highly directional nature of the L-mode scattering, and the low density of states, it is not surprising, then, that the second-sound velocity is close to $v_d/\sqrt{3}$.

In summary, we have observed the transition from ballistic phonon to second-sound propagation in bismuth, with a saturation velocity independent of orientation and equal to $v_d/\sqrt{3}$. The velocity curve (as a function of temperature) for the second-sound mode along the C_3 axis was found to yield a T^{-4} dependence for the normal-process relaxation time τ_N. Finally, we believe we have seen a manifestation of hole–L-phonon scattering along the long axis of the ellipsoid. Electron-phonon scattering along the bisectrix was found to be considerably weaker, consistent with our theoretical estimates.

We would like to thank M. Chin and J. P. Garno for their superb technical assistance, and S. Geschwind and J. M. Rowell for their support and critical reading of the manuscript.

[1]S. Shalyt, J. Phys. (U.S.S.R.) 8, 315 (1944); G. K. White and S. B. Woods, Phil. Mag. 3, 342 (1958).

[2]C. R. Brown and P. W. Matthews, Can. J. Phys. 48, 1200 (1970).

[3]V. N. Kopylov and L. P. Mezhov-Deglin, Pis'ma Zh. Eksp. Teor. Fiz. 14, 32 (1971) [JETP Lett. 14, 21 (1971)].

[4]C. C. Ackerman and R. A. Guyer, Ann. Phys. (New York) 50, 128 (1968). This paper is a review of the theoretical and experimental work on second sound in solid He^4.

[5]See Ref. 4 and C. C. Ackerman and W. C. Overton, Jr., Phys. Rev. Lett. 22, 764 (1969), for data on solid He^3.

[6]T. F. McNelly, S. J. Rogers, D. J. Channin, R. J. Rollefson, W. M. Goubau, G. E. Schmidt, J. A. Krumhansl, and R. O. Pohl, Phys. Rev. Lett. 25, 26 (1970). For detailed accounts on NaF, see H. E. Jackson and C. T. Walker, Phys. Rev. B 3, 1428 (1971); S. J. Rogers, *ibid.* 3, 1440 (1971).

[7]J. N. Fox, J. U. Trefney, J. Buchanan, L. Shen, and B. Bertman, Phys. Rev. Lett. 28, 16 (1972).

[8]For a recent review see R. J. von Gutfeld, in *Physical Acoustics*, edited by W. P. Mason (Academic, New York, 1968), Vol. 5, p. 233.

[9]Y. Eckstein, A. W. Lawson, and S. H. Reneker, J. Appl. Phys. 31, 1534 (1960).

[10]L. D. Armstrong and H. Grayson-Smith, Can. J. Res. 27A, 9 (1949).

[11]M. E. Kuznetsov, V. S. Oskotskii, V. I. Pol'shin, and S. S. Shalyt, Zh. Eksp. Teor. Fiz. 57, 1112 (1969)

[Sov. Phys. JETP 30, 607 (1970)].
[12]C. Herring, Phys. Rev. 95, 954 (1954).
[13]R. C. Dynes and V. Narayanamurti, Phys. Rev. B (to be published).
[14]R. N. Bhargava, Phys. Rev. 156, 785 (1967).
[15]J. M. Ziman, Phil. Mag. 1, 191 (1956).

Systematics and Fine Structure of Coulomb Displacement Energies

H. Seitz, S. A. A. Zaidi, and R. Bigler
*Center for Nuclear Studies, The University of Texas, Austin, Texas 78712**
(Received 5 April 1972)

Energies of isobaric-analog resonances in proton scattering on magic, transitional, and strongly deformed nuclei have been measured with an accuracy of about 15 keV. A simple phenomenological formula describes the deduced Coulomb displacement energies of magic nuclei in the range $A=48$ to 208 with an average deviation of 8 keV. Deviations from this formula for nonmagic nuclei are explained by the effect of nuclear deformation.

We have measured one or more resonances in the reactions ^{88}Sr(p,p), ^{90}Ar(p,p), ^{140}Ce(p,p), ^{141}Pr(p,p), ^{142}Nd(p,p), ^{144}Sm(p,p), and ^{208}Pb(p,p), using the proton beam of The University of Texas three-stage tandem accelerator and cooled semiconductor detectors. Considerable effort was made to obtain an accurate energy calibration of the analyzing magnet. The resonances were analyzed with the Breit-Wigner formula by methods described by Seitz.[1] Energies from excitation functions at several angles were averaged for each resonance. We found agreement with other values for ^{88}Sr,[2] for ^{140}Ce,[3,4] for ^{142}Nd,[5] for ^{144}Sm,[6] and for ^{208}Pb,[7] within the accuracy of about 15 keV. The excitation curves on ^{90}Zr[8,9] had to be shifted slightly to agree with our measured resonance energies. Energies of all strong and well-separated resonances were combined with the most accurate Q values of the corresponding (d,p) reaction presently available[10,11] to give the Coulomb displacement energies;

$$E_D = E_{\mathrm{res}}^{\mathrm{c.m.}} + Q(d,p) + 2.225 \text{ MeV}. \quad (1)$$

The average energies $\bar{E}_D$ for the above-mentioned nuclei are given in Table I, together with the energies for ^{130}Ba-^{139}La derived by Seitz *et al.*[12] and for ^{49}Ca-^{49}Sc.[13] The theoretical energies, given in Table I, were calculated from the formula

$$\bar{E}_D = \frac{aZ}{A^{1/3}} + b + [1-(-1)^z]\frac{60}{N-Z} - \frac{86\,Z}{At}, \quad (2)$$

where $a = 1394.1$ keV and $b = -416$ keV have been adjusted by a least-squares fit. All terms are given in keV. Because of the experimental errors in $\bar{E}_D$, formula (2) is accurate to about 20 keV, whereas a and b separately are only accurate to ± 3 and ± 40 keV, respectively. The first term in this formula describes the direct and the second, mainly the exchange Coulomb energy. The third term describes the Coulomb pairing interaction,[14] which is zero, except for odd-Z nuclei, and almost negligible for heavy odd-Z nuclei. The last term is an approximation to the Coulomb spin-orbit term,[15] where we have set for the nuclear radius $R = 1.2\,A^{1/3}$, and $t = \langle\langle \vec{l}\cdot\vec{\sigma} \rangle\rangle$. For the expectation values $\langle l\cdot\sigma\rangle$ we have

$$\langle \vec{l}\cdot\vec{\sigma} \rangle = \begin{cases} l \text{ for } j > l, \\ -(l+1) \text{ for } j < l. \end{cases}$$

These values are averaged over the $2T+1$ neutron orbits, which constitute the analog state in a shell-model description, to give t. In the case of the closed-shell nuclei considered here, the shell model gives very reliable configurations for the analog states, since other configurations would conflict with well-known level orders. For-

TABLE I. Comparison of experimental and theoretical displacement energies for spherical nuclei.

Analog pair	E_D^{expt} (MeV ± keV)	E_D^{theor} (MeV)	Deviation (keV)
^{49}Ca^{49}Sc	7.094 ± 11	7.103	9
^{89}Sr^{89}Y	11.337 ± 25	11.344	7
^{91}Zr^{91}Nb	11.856 ± 28	11.846	−10
^{139}Ba^{139}La	14.650 ± 15	14.640	−10
^{141}Ce^{141}Pr	15.097 ± 15	15.091	−6
^{142}Pr^{142}Nd	15.315 ± 12	15.317	2
^{143}Nd^{143}Pm	15.540 ± 16	15.536	−4
^{145}Sm^{145}Eu	15.974 ± 15	15.965	−9
^{209}Pb^{209}Bi	18.811 ± 19	15.830	19